Computer Assisted Mechanics and Engineering Sciences, 10: 431–452, 2003.

General time-dependent analysis with the frequency-domain hybrid boundary element method

Ney Augusto Dumont[1] and Ricardo A. P. Chaves[2]
[1] *Civil Engineering Department*
Pontifícia Universidade Católica do Rio de Janeiro (PUC-Rio)
22453-900 Rio de Janeiro, Brazil, e-mail: dumont@civ.puc-rio.br
[2] *Graduate student*

(Received September 11, 2003)

The paper presents an attempt to consolidate a formulation for the general analysis of the dynamic response of elastic systems. Based on the mode-superposition method, a set of coupled, higher-order differential equations of motion is transformed into a set of uncoupled second order differential equations, which may be integrated by means of standard procedures. The first motivation for these theoretical developments is the hybrid boundary element method, a generalization of T. H. H. Pian's previous achievements for finite elements which, requiring only boundary integrals, yields a stiffness matrix for arbitrary domain shapes and any number of degrees of freedom. The method is also an extension of a formulation introduced by J. S. Przemieniecki, for the free vibration analysis of bar and beam elements based on a power series of frequencies, that handles constrained and unconstrained structures, non-homogeneous initial conditions given as nodal values as well as prescribed domain fields (including rigid body movement), forced time-dependent displacements, and general domain forces (other than inertial forces).

1. Introduction

More than three decades ago, Przemieniecki [1] introduced a formulation for the free vibration analysis of bar and beam elements based on a power series of frequencies. Recently, this formulation was generalized for the analysis of the dynamic response of elastic systems submitted to arbitrary nodal loads and initial displacements. Based on the mode-superposition method, a set of coupled, higher-order differential equations of motion is transformed into a set of uncoupled second order differential equations, which may be integrated by means of standard procedures. The motivation for these theoretical developments is the hybrid boundary element method, which has been developed for time-dependent as well as frequency-dependent problems. This formulation, as a generalization of Pian's previous achievements for finite elements [2], yields a stiffness matrix defined by boundary integrals, for arbitrary domain shapes and degrees of freedom. The use of higher-order frequency terms drastically improves numerical accuracy. The modal assessment of the dynamic problem introduced here is applicable to any type of finite element for which a generalized stiffness matrix is available.

The paper presents an attempt to consolidate this boundary-only theoretical formulation, in which a series of particular cases are conceptually outlined and numerically assessed: constrained and unconstrained structures; initial displacements and velocities as nodal values, as well as prescribed domain fields (including rigid body movement); forced time-dependent displacements; self-weight and domain forces other than inertial forces; and evaluation of results at internal points [3, 4]. The paper also briefly reviews a novel formulation – the simplified hybrid boundary element method – for which the time-consuming evaluation of a flexibility matrix is no longer required. Although this simplified formulation lacks the complete variational consistency of the original method, results are extremely accurate [5]. Several academic examples for 2D problems of potential illustrate the developments.

2. Problem formulation

The time effect to be considered in the theoretical outline is due to the inertia of an elastic body [6]. One is attempting to find the displacement field u_i with a corresponding stress field σ_{ij} that satisfies the dynamic partial differential equation,

$$\sigma_{ji,j} + b_i - \rho \ddot{u}_i^c = 0 \text{ in } \Omega, \tag{1}$$

in the domain Ω, for body forces b_i and specific body mass density ρ. Subscripts i and j may assume values 1, 2 and 3, as referred to global coordinates x, y and z, respectively. A subscript after a comma denotes derivative with respect to the corresponding coordinate direction. Repeated indices indicate a three-term summation, in the general case of three-dimension problems. A dot indicates derivative with respect to time.

The displacements must satisfy the boundary condition,

$$u_i = \overline{u}_i \quad \text{along} \quad \Gamma_u, \tag{2}$$

for prescribed boundary displacements $\overline{u}_i$. Moreover, the stress field must be in equilibrium with prescribed forces t_i along the complementary part Γ_σ of the boundary:

$$\sigma_{ij}\eta_j = \overline{t}_i \quad \text{along} \quad \Gamma_\sigma. \tag{3}$$

A solution satisfying exactly all three equations above is possible only in certain particular cases. In the present hybrid formulation, one assumes that a displacement field,

$$\widetilde{u} = u_{im} d_m(t) \quad \text{along} \quad \Gamma \quad \text{such that} \quad \widetilde{u}_i = \overline{u}_i \quad \text{along} \quad \Gamma_u \tag{4}$$

is known along the boundary in terms of polynomial interpolation functions u_{im} and some time-dependent nodal displacement parameters $d_m(t)$, as it is usually done in other numerical methods. One also assumes a different displacement field,

$$u_i^f = u_i^* + u_i^b, \tag{5}$$

for the entire domain, in such a way that the dynamic equilibrium Eq. (1) is identically satisfied. It means that one can define an arbitrary particular solution u_i^b, such that the corresponding stress field σ_{ij}^b satisfies the equation,

$$\sigma_{ji,j}^b + b_i - \rho \ddot{u}_i^b = 0 \text{ in } \Omega, \tag{6}$$

and, most important, it means that one can find a homogeneous solution u_i^* with corresponding stress field σ_{ij}^*:

$$\sigma_{ji,j}^* - \rho \ddot{u}_i^* = 0 \text{ in } \Omega. \tag{7}$$

This characterizes a fundamental solution,

$$\begin{aligned} u_i^* &= u_{im}^*(t) p_m^*(t), \\ \sigma_{ij}^* &= \sigma_{ijm}^*(t) p_m^*(t), \end{aligned} \tag{8}$$

to be obtained in terms of some time-dependent nodal force parameters $p_m^*(t)$, in which the subscript m refers to each one of the degrees of freedom of the discretized model.

3. Outline of the hybrid boundary element method

The hybrid boundary element method, as introduced in 1987 as a generalization of the concepts developed by T. H. H. Pian in the finite element method [7, 8], only requires evaluation of integrals along the boundary, since it uses fundamental solutions of the conventional boundary element method as domain interpolation functions. The method considers an arbitrarily shaped domain as a single finite macro-element with as many boundary degrees of freedom as desired. The price for such an elegant and powerful formulation is the necessity of forming a flexibility matrix, which requires the evaluation of integrals along the entire boundary. However, accuracy of results, applicability, simplicity in case of some particular problems, and ease of post-processing results seem to more than compensate for some additional computational cost. The hybrid boundary element method has been successfully applied to a wide variety of potential and elasticity problems, including time-dependent problems and fracture mechanics [9–12].

Given the assumptions of Section 2, one shall look for a means of relating the fields $\widetilde{u}_i$, defined by Eq. (4) along Γ, and u_i^*, defined in Ω by Eqs. (5)–(8), in such a way that Eq. (3) is best satisfied. This may be achieved by means of a variational principle, as outlined in [6] in terms of the Hellinger–Reissner potential, generalized for time-dependent problems,

$$\int_{t_1}^{t_2} \left[-\int_\Omega \left(\delta\sigma^f_{ji,j} - \rho\delta\ddot{u}^f_i\right)\left(u^f_i - \widetilde{u}_i\right) \mathrm{d}\Omega + \int_\Gamma \delta\sigma^f_{ji}\eta_j \left(u^f_i - \widetilde{u}_i\right) \mathrm{d}\Gamma \right. \\ \left. + \int_\Omega \delta\widetilde{u}_i \left(\sigma^f_{ji,j} + b_i - \rho\ddot{u}^f_i\right) \mathrm{d}\Omega - \int_\Gamma \delta\widetilde{u}_i \left(\sigma^f_{ji}\eta_j - \bar{t}_i\right) \mathrm{d}\Gamma \right] \mathrm{d}t = 0, \tag{9}$$

in which one assumes as necessary variational prerequisites that $\delta\widetilde{u}_i = 0$ along Γ_u and that $\delta u_i^* = 0$ at both time interval extremities t_1 and t_2.

After interpolation of the variables $\widetilde{u}_i$, according to Eq. (4), as well as u_i^* and σ_{ij}^*, according to Eq. (8), one arrives at the expression, for a given time instant t:

$$\delta\mathbf{p}^{*\mathrm{T}} \left(\mathbf{F}\mathbf{p}^* - \mathbf{H}\mathbf{d} + \mathbf{b}\right) - \delta\mathbf{d}^{\mathrm{T}} \left(\mathbf{H}^{\mathrm{T}}\mathbf{p}^* + \mathbf{p}^b - \mathbf{p}\right) = \mathbf{0}. \tag{10}$$

This equation is expressed in matrix notation, for convenience. The quantities $\mathbf{p}^*$ and $\mathbf{d}$ are vectors containing the nodal parameters p_m^* and d_m, respectively – the primary unknowns of the problem. The symmetric flexibility matrix $\mathbf{F}$, the kinematic transformation matrix $\mathbf{H}$ and the vector $\mathbf{b}$ of nodal displacements equivalent to body forces may be defined in terms of boundary integrals as

$$\begin{bmatrix} \mathbf{F} \\ \mathbf{H}^{\mathrm{T}} \\ \mathbf{b}^{\mathrm{T}} \end{bmatrix} \equiv \begin{bmatrix} F_{mn} \\ H_{mn} \\ b_m \end{bmatrix} = \int_\Gamma \begin{Bmatrix} u^*_{in} \\ u_{in} \\ u^b_i \end{Bmatrix} \left\langle \sigma^*_{ijm}\eta_j \right\rangle \mathrm{d}\Gamma + \begin{Bmatrix} u^*_{in} \\ u_{in} \\ u^b_i \end{Bmatrix} \left\langle \delta_{im} \right\rangle. \tag{11}$$

Owing to the singularity of the fundamental solution, the boundary integrals represented in equations above are singular and have to be aligned into a Cauchy principal value and a discontinuous term. Related to this singularity, a generalized Kronecker delta is introduced, meaning that $\delta_{im} = 0$ in general, except if the indices i and m refer to the same degree of freedom, when $\delta_{im} = 1$. This singularity will be addressed in Subsection 3.1.

In Eq. (10), $\mathbf{p}^b$ and $\mathbf{p}$ are vectors of nodal forces equivalent to body forces b_i and traction forces $\bar{t}_i$, respectively, defined as,

$$\left[\mathbf{p}^b \ \mathbf{p}\right] \equiv \left[p^b_m \ p_m\right] = \int_\Gamma \{u_{im}\} \left\langle \sigma^b_{ji}\eta_j \ \bar{t}_i \right\rangle \mathrm{d}\Gamma. \tag{12}$$

Moreover, virtual work considerations [13] enable writing,

$$\mathbf{b} = \mathbf{H}\mathbf{d}^b, \tag{13}$$

in which $\mathbf{d}^b$ are displacements u_i^b measured directly at the boundary points.

For arbitrary values of $\delta\mathbf{p}^*$ and $\delta\mathbf{d}$, Eq. (10) becomes,

$$\mathbf{F}\mathbf{p}^* = \mathbf{H}\left(\mathbf{d} - \mathbf{d}^b\right), \tag{14}$$

$$\mathbf{H}^{\mathrm{T}}\mathbf{p}^* = \mathbf{p} - \mathbf{p}^b \tag{15}$$

or

$$\mathbf{H}^{\mathrm{T}}\mathbf{F}^{-1}\mathbf{H}\left(\mathbf{d} - \mathbf{d}^b\right) = \mathbf{p} - \mathbf{p}^b, \tag{16}$$

in which

$$\mathbf{H}^{\mathrm{T}}\mathbf{F}^{-1}\mathbf{H} = \mathbf{K}, \tag{17}$$

constitutes a symmetric, positive semi-definite stiffness matrix that transforms nodal displacements $\mathbf{d}$ into nodal forces in equilibrium with the set of equivalent nodal forces defined at the right-hand side of Eq. (16).

The numerical implementation of this formulation for a time-dependent fundamental solution is very complicated, since a singularity with respect to time has to be considered. However, harmonic as well as general transient problems may be considered in the frame of a frequency-domain formulation, as outlined in Sections 6 and 7.

3.1. Evaluation of coefficients about the main diagonal of matrix F

Equations (10)–(17), as established above for time-dependent problems, are formally the same ones obtained for static problems [7, 8]. Splitting the fundamental solution into time-independent and time-dependent terms,

$$\begin{aligned} u_i^* &= [u_{0im}^* + u_{im}^*(t)]\, p_m^*(t), \\ \sigma_{ij}^* &= [\sigma_{0ijm}^* + \sigma_{ijm}^*(t)]\, p_m^*(t), \end{aligned} \tag{18}$$

one may redefine the matrices $\mathbf{F}$ and $\mathbf{H}$ as:

$$\mathbf{F} = \mathbf{F}_0 + \mathbf{F}(t), \tag{19}$$

$$\mathbf{H} = \mathbf{H}_0 + \mathbf{H}(t). \tag{20}$$

The evaluation of $\mathbf{F}(t)$ and $\mathbf{H}(t)$ by means of the integrals indicated in Eq. (11) offers no mathematical difficulty. On the other hand, coefficients about the main diagonal of the static flexibility matrix $\mathbf{F}_0$, for m and n referring to the same node, cannot be evaluated by means of an integral. This mathematical impossibility is consistent with the assumption that the nodal point is situated outside the domain Ω, although infinitely close to it. The determination of these elements has to be carried out indirectly by requiring that $\mathbf{F}_0$ satisfies the orthogonality criterion [7, 8],

$$\mathbf{F}_0\mathbf{V} = \mathbf{0}, \tag{21}$$

in which $\mathbf{V}$ is a basis of eigenvectors corresponding to zero-eigenvalues of the matrix $\mathbf{H}_0^{\mathrm{T}}$,

$$\mathbf{H}_0^{\mathrm{T}}\mathbf{V} = \mathbf{0}, \tag{22}$$

as developed in Subsection 4.1.

4. Outline of the simplified hybrid boundary element method

In the following, one introduces a novel formulation – the simplified hybrid boundary element method – as applied to transient problems. In this simplified version, the time-consuming evaluation of the flexibility matrix $\mathbf{F}$ defined in Section 3 is no longer required. However, as a price of simplification, one gives up the complete variational consistency of the original method. As it shall be outlined, the equations of this method may be settled on bases that are completely independent from all previously developed boundary element approaches [14–17], although keeping conceptual affinity with the variational formulation just presented. In fact, as it will be outlined in Section 5, the extension of the (variational) hybrid boundary element method to unbounded regions and to multiply connected domains has become possible only after the full development of this simplified version.

4.1. Nodal force equilibrium in terms of virtual work

A set of equations relating equivalent nodal forces acting on the boundary to the concentrated forces $\mathbf{p}^*$ was obtained in Eq. (15) in the frame of the hybrid boundary element method, based on the Hellinger–Reissner potential. However, in this Section the same result is obtained in a simpler way. Given a virtual field of displacements $\delta\widetilde{u}_i$, such that,

$$\delta\widetilde{\varepsilon}_{ij} = \frac{1}{2}\left(\delta\widetilde{u}_{i,j} + \delta\widetilde{u}_{j,i}\right) \text{ in } \Omega \tag{23}$$

and,

$$\delta\widetilde{u}_i = 0 \text{ in } \Gamma_u. \tag{24}$$

Equations (1)–(3) are equivalent to the virtual work statement,

$$\int_\Omega \left(\sigma^*_{ij} + \sigma^b_{ij}\right)\delta\widetilde{u}_{i,j}\mathrm{d}\Omega = \int_\Omega \left(b_i - \rho\ddot{u}^*_i - \rho\ddot{u}^b_i\right)\delta\widetilde{u}_i\mathrm{d}\Omega + \int_\Gamma \bar{t}_i\delta\widetilde{u}_i\mathrm{d}\Gamma, \tag{25}$$

assuming that the stress tensor is symmetric. Integration by parts of the term at the left-hand side of this equation and application of Green's theorem yield,

$$\int_\Gamma \sigma^*_{ji}\eta_j\delta\widetilde{u}_i\mathrm{d}\Gamma - \int_\Omega \left(\sigma^*_{ji,j} - \rho\ddot{u}^*_i\right)\delta\widetilde{u}_i\mathrm{d}\Omega = \int_\Gamma \bar{t}_i\delta\widetilde{u}_i\mathrm{d}\Gamma - \int_\Gamma \sigma^b_{ji}\eta_j\delta\widetilde{u}_i\mathrm{d}\Gamma \tag{26}$$

or, substituting for $\delta\widetilde{u}_i$ and σ^*_{ij} according to Eqs. (4) and (8), respectively,

$$\begin{aligned}\delta d_n \left[\int_\Gamma \sigma^*_{ijm}\eta_j u_{in}\mathrm{d}\Gamma - \int_\Omega \left(\sigma^*_{ijm,j} - \rho\ddot{u}^*_{im}\right)u_{in}\mathrm{d}\Omega\right] p^*_m \\ = \delta d_n \left(\int_\Gamma t_i u_{in}\mathrm{d}\Gamma - \int_\Gamma \sigma^b_{ji}\eta_j u_{in}\mathrm{d}\Gamma\right).\end{aligned} \tag{27}$$

Then, for arbitrary nodal displacements $\delta\mathbf{d} \equiv \delta d_n$ one obtains the matrix equilibrium equation,

$$\mathbf{H}^{\mathrm{T}}\mathbf{p}^* = \mathbf{p} - \mathbf{p}^b, \tag{28}$$

the same as Eq. (15), in which the transpose of the kinematic transformation matrix $\mathbf{H}$, already defined in Eq. (11) – and which also appears in the frame of the conventional boundary element method, although with a different physical meaning – is an equilibrium matrix that transforms singular forces $\mathbf{p}^*$ into equivalent nodal forces $\mathbf{p} - \mathbf{p}^b$, also already defined in Eqs. (12).

The boundary integral indicated in Eq. (11) is singular, as stated in Section 3. It has to be evaluated in terms of a Cauchy principal value (as a sum of finite-part integrals) plus a local

discontinuous term. Since this singularity only affects the terms about the main diagonal (for d_n and p_m^* referring to the same nodal point), these terms may also be obtained indirectly, in the frame of the orthogonality property of the equilibrium matrix $\mathbf{H}$, for a bounded domain. In fact, one may aligned this matrix into time-dependent and time-independent matrices:

$$\mathbf{H} = \mathbf{H}_0 + \mathbf{H}(t). \tag{29}$$

Then, $\mathbf{H}_0$ corresponds to the static formulation, so that,

$$\mathbf{H}_0\mathbf{W} = \mathbf{0}, \tag{30}$$

in which $\mathbf{W}$ is a normal basis of the rigid body displacements. The demonstration of this spectral property is straightforward. The following relation may also be demonstrated for the time-independent part of the applied equivalent nodal forces of Eq. (28):

$$\mathbf{W}^{\mathrm{T}}\left(\mathbf{p}_0 - \mathbf{p}_0^b\right) = \mathbf{0}. \tag{31}$$

This means that, although matrix $\mathbf{H}_0$ is singular, the equation system (28) is consistent and must have a unique solution, even if particularized to static problems. An obvious consequence of the orthogonality property (30) is that there also must be a normal basis $\mathbf{V}$ of vectors such that,

$$\mathbf{H}_0^{\mathrm{T}}\mathbf{V} = \mathbf{0}, \tag{32}$$

as in Eq. (22). Due to the orthogonality properties (30)–(32), the singular forces $\mathbf{p}_0^*$ in Eq. (28), considered as the static case, must satisfy also the orthogonality condition:

$$\mathbf{V}^{\mathrm{T}}\mathbf{p}_0^* = \mathbf{0}. \tag{33}$$

This is consistent with Eq. (21).

4.2. Nodal displacement compatibility

The displacements in the domain of an elastic body are expressed according to Eqs. (5) and (8) as,

$$u_i^f = u_{im}^* p_m^* + u_i^b \text{ in } \Omega, \tag{34}$$

in which u_{im}^* is the displacement fundamental solution corresponding to the concentrated nodal forces p_m^*, and u_i^b are the displacements corresponding to the particular solution. Eq. (34) is valid for the domain Ω, as a consequence of the stress assumption therein, whereas Eq. (4) is assumed for the displacements along the boundary Γ. However, one may enforce that both assumptions coincide at the nodal points. In matrix notation,

$$\mathbf{d} = \mathbf{U}^*\mathbf{p}^* + \mathbf{d}^b, \tag{35}$$

where $\mathbf{U}^* \equiv U_{mn}^*$ and $\mathbf{d}^b \equiv u_m^b$ are the displacements measured at the nodal points, as related to the fundamental solution and the particular solution, respectively. Matrix $\mathbf{U}^* \equiv U_{mn}^*$, of nodal displacements corresponding to the fundamental solution, is symmetric by construction. However, the coefficients that refer to forces and displacements applied and measured at the same nodal point cannot be determined directly, since a singular fundamental solution is not determined at the point of application of the concentrated force. Strictly speaking, as stated for the stress assumption, each concentrated force is applied just outside the domain, at points that are infinitely close, but not part of the domain. As a consequence, if Eq. (35) is to have any use, the elements about the main diagonal of $\mathbf{U}^*$ must be obtained indirectly by means of some property or assumption still to be defined.

4.3. Evaluation of the coefficients about the main diagonal of $\mathbf{U}^*$

In fact, one may aligned matrix $\mathbf{U}^*$ into time-dependent and time-independent matrices:

$$\mathbf{U}^* = \mathbf{U}_0^* + \mathbf{U}(t), \tag{36}$$

in which $\mathbf{U}(t)$ is completely determined (with zero values for the block-diagonal coefficients). For evaluation of the main-diagonal coefficients of $\mathbf{U}_0^*$, one applies Eq. (34) to the static case, rewritten in an equivalent, although more convenient expression [16],

$$u_{0i}^f = (u_{0im}^* + u_{is}^r C_{sm})\, p_{0m}^* + u_{0i}^b \text{ in } \Omega, \tag{37}$$

where the term in brackets – the displacement fundamental solution and some rigid body displacements – is assumed to be orthogonal to rigid body motions. This substantiates the fact that, in the static case, the interaction between the primary unknowns of the problem – the concentrated nodal forces $\mathbf{p}_0^*$ and the nodal displacements $\mathbf{d}_0$ – does only occur in terms of strain energy and equilibrated forces, as established by Eqs. (30) and (31). In Eq. (37), u_{is}^r is a set of rigid body functions normalized (for simplicity) in such a way so as to yield matrix $\mathbf{W}$ of Eq. (30), when evaluated at the nodal points. A criterion for finding the matrix of constants C_{sm} is the orthogonality condition,

$$\int_\Gamma u_{ir}^r\, (u_{0im}^* + u_{is}^r C_{sm})\, \mathrm{d}\Gamma\; p_{0m}^* = 0, \tag{38}$$

valid for any p_{0m}^*. Then, it results for $\mathbf{C} \equiv C_{sm}$,

$$\mathbf{C}^* + \mathbf{C}^r \mathbf{C} = 0 \quad \Rightarrow \quad \mathbf{C} = -\,(\mathbf{C}^r)^{-1}\, \mathbf{C}^*, \tag{39}$$

in which,

$$\mathbf{C}^r \equiv C_{rs}^r = \int_\Gamma u_{ir}^r u_{is}^r \mathrm{d}\Omega \qquad \text{and} \qquad \mathbf{C}^* \equiv C_{rm}^* = \int_\Gamma u_{ir}^r u_{0im}^* \mathrm{d}\Gamma. \tag{40}$$

$\mathbf{C}^r$ is a square, symmetric positive definite matrix, the order of which is the number of rigid body displacements. $\mathbf{C}^*$ has as many rows as the number of rigid body displacements and as many columns as the number of degrees of freedom.

After the matrix C_{sm} is obtained by Eqs. (38)–(40), the term in brackets in Eq. (37) turns out to be orthogonal to rigid body displacements. When applied to the nodal points,

$$\mathbf{d}_0 = (\mathbf{U}_0^* + \mathbf{W}\mathbf{C})\, \mathbf{p}_0^*. \tag{41}$$

This equation only holds for nodal displacements $\mathbf{d}_0$ and concentrated forces $\mathbf{p}_0^*$ orthogonal to $\mathbf{W}$ and $\mathbf{V}$, respectively. As a consequence, one has the orthogonality condition,

$$(\mathbf{U}_0^* + \mathbf{W}\mathbf{C})\, \mathbf{V} = \mathbf{0}, \tag{42}$$

with which it is possible to evaluate the coefficients about the main diagonal of $\mathbf{U}_0^*$. It may be demonstrated that the product $\mathbf{CV}$ in Eq. (42) is unique, independently of the normal basis $\mathbf{V}$ one might have chosen [13]. For potential problems, this equation results in a set of uncoupled equations for each diagonal coefficient of $\mathbf{U}_0^*$. For elasticity problems, it results in separate subsets of coupled equations for the coefficients of each nodal point, which can only be solved in terms of least squares. This is the exact procedure introduced by Dumont [7, 8] for evaluating the coefficients about the main diagonal of the flexibility matrix $\mathbf{F}$ obtained in the hybrid boundary element method, for static problems. One verifies numerically that the least squares residues tend to vanish as the number of boundary nodal points increases.

4.4. A stiffness-type matrix

Eliminating $\mathbf{p}^*$ in Eqs. (28) and (35), one obtains,

$$\mathbf{H}^{\mathrm{T}} (\mathbf{U}^*)^{-1} \left(\mathbf{d} - \mathbf{d}^b\right) = \mathbf{p} - \mathbf{p}^b, \tag{43}$$

in which,

$$\mathbf{K} = \mathbf{H}^{\mathrm{T}} (\mathbf{U}^*)^{-1}, \tag{44}$$

is a stiffness-type matrix. Since Eq. (35) is formulated on the basis of a non-variational approach, $\mathbf{K}$ is not necessarily symmetric. However, $\mathbf{K}$ tends to become symmetric with increasing mesh refinement [13]. With slight modifications, the developments presented in this paper are also valid for infinite domains (next Subsection).

The present research line on boundary elements was started, in 1986, with the investigation of the non-variational character of conventional boundary element methods and showing that the stiffness-like matrix one obtains in the collocation approach cannot be symmetrized without the perpetration of a serious mechanical mistake [7, 18]. Consistently with this criticism, a variational formulation was published [8], which resulted coincident with the Hellinger–Reissner potential, although more general than the earlier proposition for finite elements made by Pian [2]. Now, ironically, one arrives at a simplified version of this variational approach, which does not lead to a stiffness matrix, Eq. (44), that is symmetric by construction. Although still preliminary, a careful investigation has led to the conclusion that the lack of symmetry of the stiffness matrix $\mathbf{K}$ in Eq. (44) is within the range of the discretization errors [13]. Moreover, the static term $\mathbf{K}_0$ implicit in $\mathbf{K}$ is by construction orthogonal to rigid body motions. Unfortunately, one has to content oneself with this short explanation, in the frame of the present paper, just asserting that, instead of Eq. (44), one may use the symmetrized form,

$$\mathbf{K} = \frac{1}{2}\left[\mathbf{H}^{\mathrm{T}} (\mathbf{U}^*)^{-1} + (\mathbf{U}^*)^{-1} \mathbf{H}\right]. \tag{45}$$

In the following sections, one always refers to the stiffness matrix $\mathbf{K}$ obtained in Eq. (17), since modifications for taking into account the simplified method are straightforward.

5. Application of the methods to unbounded regions

The feasibility of both variational (Section 3) and simplified (Section 4) hybrid boundary element methods relies on the possibility of evaluating the elements about the main diagonal of matrices $\mathbf{F}_0$ and $\mathbf{U}_0^*$, according to the orthogonality Eqs. (21) and (42), respectively. However, this is only possible if the submatrices about the main diagonal of the orthogonal projector $\mathbf{V}\mathbf{V}^{\mathrm{T}}$, which refer to each nodal point, are all non-singular. It may be demonstrated that Eqs. (21) and (42) are applicable in both cases of simply connected, finite and infinite domains. In case of a multiply connected domain, on the other hand, it may be demonstrated that singularities or strong ill-conditioning unavoidably occur in the block-diagonal submatrices of the orthogonal projector $\mathbf{V}\mathbf{V}^{\mathrm{T}}$, for nodal points along interior subboundaries. Both cases of singularity and ill-conditioning are physically explainable as a topological lack of correspondence between the bases $\mathbf{W}$ and $\mathbf{V}$. The theoretical discussion of this subject belongs to the fundamentals of the hybrid boundary element method and is being prepared for publication. Nevertheless, the present method can be applied to a multiply connected domain, if one deals with the problem by superposing solutions for finite and infinite domains.

Equations (21) and (42) are not directly applicable for the consideration of infinite domains, since one can exclude neither rigid body displacements nor unbalanced forces from the energy considerations, when dealing with this topologically different problem. Fortunately, there are some simple relations between the matrices obtained for a cavity in an infinite domain and the corresponding

matrices for the complementary bounded domain. In fact, characterizing the matrices for an infinite domain with an upper bar $\overline{(\,)}$, it is possible to demonstrate the following relations, given that one simply reverses the sense of integration in Eqs. (11),

$$\overline{\mathbf{H}}_0 = \mathbf{I} - \mathbf{H}_0, \qquad \overline{\mathbf{F}}_0 = \mathbf{U}_0^* - \mathbf{F}_0, \tag{46}$$

in which $\mathbf{I}$ is the identity matrix. From the first of Eqs. (46) together with Eq. (30) one readily obtains,

$$\overline{\mathbf{H}}_0 \mathbf{W} = \mathbf{W}, \tag{47}$$

a well known result in the boundary element literature, which is the counterpart of Eq. (30) for unbounded regions. For the flexibility matrix, on the other hand, one first adds the product $\mathbf{WC}$, for $\mathbf{C}$ given according to Eqs. (38–40), to both sides of the second of Eqs. (46):

$$(\overline{\mathbf{F}}_0 + \mathbf{WC}) = (\mathbf{U}_0^* + \mathbf{WC}) - \mathbf{F}_0. \tag{48}$$

Then, multiplying all terms of this equation by $\mathbf{V}$, it follows from Eqs. (21) and (42) that

$$(\overline{\mathbf{F}}_0 + \mathbf{WC})\,\mathbf{V} = \mathbf{0}, \tag{49}$$

which is the orthogonality condition required to evaluate the coefficients about the main diagonal of the non-singular matrix $\overline{\mathbf{F}}_0$.

Equation (49) shows that the variational and the simplified versions of the hybrid boundary element method, as presented in this paper, are interconnected. Some more conceptual considerations relating these methods and other boundary element methods are reviewed in [19].

6. Frequency-domain formulation

For the sake of arriving at a frequency formulation from the general developments of the previous sections, one first assumes that the trial solutions $\widetilde{u}_i$ along Γ, Eq. (4), and u_i^* in Ω, Eq. (8), may be expressed in terms of separate variables of space and time, for a given circular frequency of vibration ω:

$$\widetilde{u}_i = u_{im} d_m(\omega) \tau(t,\omega) \quad \text{along} \quad \Gamma, \tag{50}$$

$$u_i^* = u_{im}^*(\omega) p_m^*(\omega) \tau(t,\omega), \qquad \sigma_{ij}^* = \sigma_{ijm}^*(\omega) p_m^*(\omega) \tau(t,\omega), \tag{51}$$

where $\tau(t,\omega)$ is defined in such a way that

$$\frac{\partial^2 \tau(t,\omega)}{\partial t^2} = -\omega^2 \tau(t,\omega). \tag{52}$$

The formulation above relies on the existence of a fundamental solution, as introduced in Eq. (51), which, by definition, satisfies Eq. (7) for a given circular frequency ω [4, 6, 7]:

$$\sigma_{ij,j}^*(\omega) + \omega^2 \rho u_i^*(\omega) = 0. \tag{53}$$

The solution of this equation may be adequately expressed as

$$u_{im}^*(\omega) \leftarrow u_{im}^*(0) + u_{im}^*(\omega) \quad \text{and} \quad \sigma_{ijm}^*(\omega) \leftarrow \sigma_{ijm}^*(0) + \sigma_{ijm}^*(\omega), \tag{54}$$

in which $u_{im}^*(0)$ and $\sigma_{ijm}^*(0)$ correspond to the static fundamental solution. On the other hand, the frequency-dependent terms $u_{im}^*(\omega)$ and $\sigma_{ijm}^*(\omega)$ are by construction non-singular functions that

require no special consideration for the sake of integration in Eq. (11). For two-dimensional problems of potential, for example, the Helmholtz Eq. (53) has as solution [9, 13],

$$\theta^* = \frac{-1}{2\pi}\ln(r) + \frac{-1}{2\pi}\left[\frac{\pi}{2}\mathrm{Y}_0(kr) - \ln(r) - \left(\ln\left(\frac{k}{2}\right) + \gamma\right)\mathrm{J}_0(kr)\right]. \tag{55}$$

Then, according to Eqs. (50–52), Eqs. (14) and (15) become, for a given circular frequency ω,

$$\begin{aligned} &\mathbf{F}(\omega)\mathbf{p}^*(\omega)\tau(t,\omega) - \mathbf{H}(\omega)\left[\mathbf{d}(\omega) - \mathbf{d}^b(\omega)\right]\tau(t,\omega) = \mathbf{0}, \\ &\mathbf{H}^{\mathrm{T}}(\omega)\mathbf{p}^*(\omega)\tau(t,\omega) - \left[\mathbf{p}(\omega) - \mathbf{p}^b(\omega)\right]\tau(t,\omega) = \mathbf{0}, \end{aligned} \tag{56}$$

in which $\mathbf{p}(\omega)$, $\mathbf{p}^b(\omega)$ and $\mathbf{d}^b(\omega)$ are, according to Eqs. (12) and (13) the harmonic components of the general time-dependent vectors $\mathbf{p}$, $\mathbf{p}^b$ and $\mathbf{d}^b$, respectively.

As a consequence of writing the fundamental solution in the shape of Eq. (54), the matrices $\mathbf{F}$ and $\mathbf{H}$ above may be formally represented as,

$$\mathbf{F}(\omega) \equiv \mathbf{F}_0 + \mathbf{F}_\omega, \qquad \mathbf{H}(\omega) \equiv \mathbf{H}_0 + \mathbf{H}_\omega. \tag{57}$$

In these equations, the frequency-dependent terms $\mathbf{F}_\omega$ and $\mathbf{H}_\omega$ involve no singularities. The terms $\mathbf{F}_0$ and $\mathbf{H}_0$ correspond to the matrices of the static formulation, with integration singularities that can be dealt with adequately. Moreover, the terms about the main diagonal of $\mathbf{F}_0$, which cannot be evaluated by means of the integration indicated in Eq. (11), may be obtained by means of spectral properties that affect exclusively the static formulation, for both cases of finite and infinite regions, according to the developments of the previous sections.

7. General time-dependent analysis in the frequency domain

Instead of formulating a problem for a given frequency, one may express the fundamental solution, Eq. (54), as a truncated power series of frequencies. For example, Eq. (55) would read:

$$\begin{aligned} \theta^* = -\frac{\ln(r)}{2\pi} + \frac{k^2r^2}{27648\pi}\Big[&(\ln(r) - 1)\,3456 - (216\ln(r) - 324)\,k^2r^2 \\ &+ (6\ln(r) - 11)\,k^4r^4\Big] + O(r^8). \end{aligned} \tag{58}$$

As a consequence, matrices $\mathbf{F}$ and $\mathbf{H}$, defined in Eq. (11), as well as $\mathbf{K}$, defined in either Eqs. (17) or (45), become also power series of frequencies with an arbitrary number n of terms [9, 13]:

$$\mathbf{F} = \sum_{i=0}^{n} \omega^{2i}\mathbf{F}_i, \qquad \mathbf{H} = \sum_{i=0}^{n} \omega^{2i}\mathbf{H}_i, \qquad \mathbf{K} = \sum_{i=0}^{n} \omega^{2i}\mathbf{K}_i. \tag{59}$$

Moreover, according to the definition of the time function $\tau(t,\omega)$ in Eq. (52), one may compose the time-dependent vector $\mathbf{d}$ of nodal displacements one is looking for as the truncated series with m terms:

$$\mathbf{d} \equiv \mathbf{d}(t) = \sum_{j=1}^{m} \mathbf{d}_j\tau(t,\omega_j). \tag{60}$$

The specific aspect of $\tau(t,\omega_j)$ in the series introduced above is not relevant in this paper.

Then, it is possible to model the behavior of a damping-free structure as:

$$\sum_{j=1}^{m}\left(\mathbf{K}_0 - \sum_{i=1}^{n}\omega_j^{2i}\mathbf{M}_i\right)\left(\mathbf{d}_j - \mathbf{d}_j^b\right)\tau(t,\omega_j) = \mathbf{p}(t) - \mathbf{p}^b(t). \tag{61}$$

In this equation, one expresses $\mathbf{K}_0$ explicitly as the stiffness matrix of the static discrete-element formulation and renames the remaining terms of the power series of $\mathbf{K}$ in Eq. (59) as generalized mass matrices $-\mathbf{M}_i$, although they constitute a blending of mass and stiffness matrices. The only exception is matrix $\mathbf{M}_1$, which corresponds to the mass matrix obtained in the conventional formulation that truncates after ω^2 [1]. The displacement vectors $\mathbf{d}_j$ are the unknowns of the problem, to be determined for applied body and traction forces, and initial nodal displacements and velocities. The number n of frequency-related matrices is arbitrary. The advantage of such a formulation based on a power series of frequencies is that it provides a more accurate fulfillment of the dynamic differential equilibrium equations of stresses at internal points of the elastic body [6, 9].

According to the definition of $\tau(t,\omega)$ in Eq. (52), Eq. (61) may be written alternatively as,

$$\left(\mathbf{K}_0 - \sum_{i=1}^{n}(-1)^i \mathbf{M}_i \frac{\partial^{2i}}{\partial t^{2i}}\right)\left(\mathbf{d} - \mathbf{d}^b\right) = \mathbf{p}(t) - \mathbf{p}^b(t), \tag{62}$$

which is a coupled set of higher-order time derivatives that makes use of the matrices obtained in the frequency formulation.

The non-linear eigenvalue problem related to Eq. (62) has the form,

$$\mathbf{K}_0\boldsymbol{\Phi} - \sum_{i=1}^{n}\mathbf{M}_i\boldsymbol{\Phi}\boldsymbol{\Omega}^{2i} = \mathbf{0}, \tag{63}$$

in which $\boldsymbol{\Omega}^2$ is a diagonal matrix with as many eigenvalues ω^2 as the number of degrees of freedom of the structure and $\boldsymbol{\Phi}$ is a matrix whose columns are the corresponding eigenvectors. This non-linear eigenvalue problem is difficult to deal with, since numerical convergence cannot be easily assured and round-off errors occur unavoidably. It is assumed that this eigenvalue problem has been solved adequately, with $\boldsymbol{\Phi}$ satisfying following general orthogonality conditions [9]:

$$\sum_{i=1}^{n}\sum_{j=i}^{n}\boldsymbol{\Omega}^{2j-2i}\boldsymbol{\Phi}^{\mathrm{T}}\mathbf{M}_j\boldsymbol{\Phi}\boldsymbol{\Omega}^{2i-2} = \mathbf{I}, \tag{64}$$

$$\left(\boldsymbol{\Phi}^{\mathrm{T}}\mathbf{K}_0\boldsymbol{\Phi} + \sum_{i=1}^{n-1}\sum_{j=1}^{n-i}\boldsymbol{\Omega}^{2i}\boldsymbol{\Phi}^{\mathrm{T}}\mathbf{M}_{j+i}\boldsymbol{\Phi}\boldsymbol{\Omega}^{2j}\right) = \boldsymbol{\Omega}^2. \tag{65}$$

In the context of a mode-superposition procedure, one may approximate the time-dependent displacements $\mathbf{d}(t)$ as a finite sum of contributions of the normalized eigenvectors $\boldsymbol{\Phi}$, according to Eqs. (64) and (65), multiplied by a vector of amplitudes $\boldsymbol{\eta} \equiv \boldsymbol{\eta}(t)$, which are the new unknowns of the problem:

$$\mathbf{d} = \boldsymbol{\Phi}\boldsymbol{\eta}. \tag{66}$$

Then, after some tedious manipulation [9], one transforms Eq. (62) into:

$$\boldsymbol{\Omega}^2\left(\boldsymbol{\eta} - \boldsymbol{\eta}^b\right) + \ddot{\boldsymbol{\eta}} - \ddot{\boldsymbol{\eta}}^b = \boldsymbol{\Phi}^{\mathrm{T}}\left(\mathbf{p} - \mathbf{p}^b\right). \tag{67}$$

This is an uncoupled system of second order differential equations in time, which may be integrated by means of standard procedures. This equation is equivalent to

$$\boldsymbol{\Omega}^2\boldsymbol{\eta} + \ddot{\boldsymbol{\eta}} = \boldsymbol{\Phi}^{\mathrm{T}}\left(\mathbf{p} - \mathbf{p}^b\right) + \boldsymbol{\Phi}^{\mathrm{T}}\left(\mathbf{K}_0 - \sum_{i=1}^{n}(-1)^i\mathbf{M}_i\frac{\partial^{2i}}{\partial t^{2i}}\right)\mathbf{d}^b. \tag{68}$$

7.1. Consideration of non-homogeneous initial conditions

For the sake of both expressing the initial displacement conditions necessary as integration constants in equations above and obtaining $\boldsymbol{\eta}^b$ from $\mathbf{d}^b$, it may be demonstrated [13] that, for the subsets $\boldsymbol{\Phi}_{\text{el}}$ and $\boldsymbol{\Omega}_{\text{el}}$ of modes and frequencies related to pure elastic deformation,

$$\boldsymbol{\eta}_{\text{el}} = \left[\boldsymbol{\Phi}_{\text{el}}^{\text{T}}\mathbf{K}_0\boldsymbol{\Phi}_{\text{el}}\right]^{-1}\boldsymbol{\Phi}_{\text{el}}^{\text{T}}\mathbf{K}_0\mathbf{d}, \tag{69}$$

whereas for the subsets $\boldsymbol{\Phi}_{\text{rig}}$ and $\boldsymbol{\Omega}_{\text{rig}} \equiv 0$ related to rigid body displacements, one has:

$$\boldsymbol{\eta}_{\text{rig}} = \boldsymbol{\Phi}_{\text{rig}}^{\text{T}}\mathbf{M}_1\mathbf{d}. \tag{70}$$

The set of uncoupled second order differential equations in time (67), together with Eqs. (69) and (70) for the consideration of initial displacements, is the transformation of Eq. (62) for the solution of a wide range of time-dependent problems on the basis of a frequency formulation.

7.2. Consideration of forced nodal displacements

When part of the nodal displacements are known functions of time, one proceeds exactly as in the conventional dynamic analysis [1, 13], rewriting Eq. (62) in terms of submatrices,

$$\left(\begin{bmatrix} \mathbf{K}_0^{pp} & \mathbf{K}_0^{pf} \\ \mathbf{K}_0^{fp} & \mathbf{K}_0^{ff} \end{bmatrix} - \sum_{i=1}^{n}(-1)^i \begin{bmatrix} \mathbf{M}_i^{pp} & \mathbf{M}_i^{pf} \\ \mathbf{M}_i^{fp} & \mathbf{M}_i^{ff} \end{bmatrix} \frac{\partial^{2i}}{\partial t^{2i}}\right) \begin{Bmatrix} (\mathbf{d}-\mathbf{d}^b)^p \\ (\mathbf{d}-\mathbf{d}^b)^f \end{Bmatrix} = \begin{Bmatrix} (\mathbf{p}-\mathbf{p}^b)^p \\ (\mathbf{p}-\mathbf{p}^b)^f \end{Bmatrix} \tag{71}$$

in which the subscripts p and f refer to *prescribed* and *free* subsets of nodal displacements, respectively. The second set of submatrix equations above may read explicitly:

$$\begin{aligned} \left(\mathbf{K}_0^{ff} - \sum_{i=1}^{n}(-1)^i\mathbf{M}_i^{ff}\frac{\partial^{2i}}{\partial t^{2i}}\right)\left(\mathbf{d}-\mathbf{d}^b\right)^f &= \left(\mathbf{p}-\mathbf{p}^b\right)^f \\ - \left(\mathbf{K}_0^{fp} - \sum_{i=1}^{n}(-1)^i\mathbf{M}_i^{fp}\frac{\partial^{2i}}{\partial t^{2i}}\right)&\left(\mathbf{d}-\mathbf{d}^b\right)^p. \end{aligned} \tag{72}$$

Since all quantities at the right-hand side of Eq. (72) are known functions of time, this equation is formally equivalent to Eq. (62), for the sake of the modal superposition procedure used to arrive at Eq. (67). Once the displacements $\mathbf{d}^f$ are obtained, after transformation of Eq. (72) in a set of uncoupled second order equations, the time-dependent reaction forces related to the prescribed nodes may be evaluated using the first set of the submatrix equations (71). A word of caution is needed concerning the numerical implementation of Eq. (72), as the higher-order derivatives in the right-hand side may lead to unreliable results if $\left(\mathbf{d}-\mathbf{d}^b\right)^p$ is not a close expression of time, but some series approximation instead [13].

7.3. Evaluation of results at internal points

In a harmonic formulation, the singular force parameters $\mathbf{p}^*(\omega)$ are obtained, according to the first of Eqs. (56), by,

$$\mathbf{p}^*(\omega) = \mathbf{S}(\omega)\left(\mathbf{d}(\omega) - \mathbf{d}^b(\omega)\right), \tag{73}$$

where $\mathbf{S}(\omega) = \mathbf{F}^{-1}(\omega)\mathbf{H}(\omega)$. For the power series of frequencies introduced in this section, according to Eqs. (59) and as illustrated in Eq. (58), the equation above is replaced by,

$$\mathbf{p}^*(\omega) \approx \sum_{i=0}^{n}\omega^{2i}\mathbf{S}_i\left(\mathbf{d}(\omega) - \mathbf{d}^b(\omega)\right), \tag{74}$$

with:

$$\sum_{i=0}^{n} \omega^{2i} \mathbf{S}_i = \left(\sum_{i=0}^{n} \omega^{2i} \mathbf{F}_i \right)^{-1} \sum_{i=0}^{n} \omega^{2i} \mathbf{H}_i. \tag{75}$$

Readers are referred to [9, 13] for the adequate evaluation of this expression, particularly concerning the matrix power series inversion, as the leading matrix $\mathbf{F}_0$ is generally singular.

For the simplified hybrid boundary element method presented in Section 4, the matrix $\mathbf{S}(\omega)$ in Eq. (73) is simply substituted by

$$\mathbf{S}(\omega) = (\mathbf{U}^*(\omega))^{-1}, \tag{76}$$

the computation of which is straightforward, as the leading term $\mathbf{U}_0^*$ of $\mathbf{U}^*(\omega)$ is not singular [13].

Transformed to the time-dependent formulation introduced in this section, and considering forced nodal displacements, for the sake of generality, Eq. (74) reads [13],

$$\mathbf{p}^*(t) = \sum_{i=0}^{n} \mathbf{S}_i^f \boldsymbol{\Phi} \boldsymbol{\Omega}^{2i} \left(\boldsymbol{\eta} - \boldsymbol{\eta}^b \right)^f + \sum_{i=0}^{n} (-1)^i \mathbf{S}_i^p \frac{\partial^{2i}}{\partial t^{2i}} \left(\mathbf{d} - \mathbf{d}^b \right)^p, \tag{77}$$

in which matrices $\mathbf{S}_i$ are aligned in submatrices related to free and prescribed nodal displacements. It is worth observing that the only higher-order derivatives involved are related to the prescribed nodal displacements, which must be evaluated as accurately as possible. The nodal displacements $\mathbf{d}^f$, evaluated at the free nodes as a particular body force solution, might be considered explicitly in the equation, in place of its modal representation, as discussed for Eq. (68). However, the configuration of Eq. (77) is more compact and elegant.

Once $\mathbf{p}^*(t)$ is evaluated, one is able to represent results at internal points. The general displacement expression in the first of Eqs. (8) and the corresponding superposition of effects in the frequency domain [13] yield:

$$\mathbf{u}^*(t) = \sum_{j=1}^{m} \sum_{i=0}^{n} \omega_j^{2i} \mathbf{u}_i^* \mathbf{p}^* \equiv \sum_{i=0}^{n} \mathbf{u}_i^* \boldsymbol{\Omega}^{2i} \mathbf{p}^*. \tag{78}$$

Notice that $\mathbf{u}^*(t)$ is a vector with as many elements as the number of degrees of freedom at a domain point (one for problems of potential, two for 2D elasticity and 3 for 3D elasticity). Also, each matrix $\mathbf{u}_i^*$ has as many rows as the number of degrees of freedom at a point and as many columns as the total number of nodal degrees of freedom. Making use of this equation, the expression for $\mathbf{u}^f$ becomes, according to Eq. (5), for the general consideration of body forces and forced nodal displacements:

$$\mathbf{u}^f(t) = \sum_{i=0}^{n} \sum_{j=0}^{i} \mathbf{u}_j^* \mathbf{S}_{i-j}^f \boldsymbol{\Phi} \boldsymbol{\Omega}^{2i} \left(\boldsymbol{\eta} - \boldsymbol{\eta}^b \right)^f + \sum_{i=0}^{n} (-1)^i \sum_{j=0}^{i} \mathbf{u}_j^* \mathbf{S}_{i-j}^p \frac{\partial^{2i}}{\partial t^{2i}} \left(\mathbf{d} - \mathbf{d}^b \right)^p + \mathbf{u}^b(t). \tag{79}$$

In this equation, coherently with the procedures for multiplication and inversion of matrix power series, only exponents of $\boldsymbol{\Omega}$ and derivatives of $\mathbf{d}$ up to $2n$ are retained in the expressions, according to Eq. (59) for the evaluation of $\mathbf{K}$, and Eq. (75). As a matter of illustration, in the absence of body forces and considering no prescribed nodal displacements, Eq. (79) becomes, for $n = 3$,

$$\begin{aligned} \mathbf{u}^f(t) = \big[& \mathbf{u}_0^* \mathbf{S}_0 \boldsymbol{\Phi} + (\mathbf{u}_0^* \mathbf{S}_1 + \mathbf{u}_1^* \mathbf{S}_0) \boldsymbol{\Phi} \boldsymbol{\Omega}^2 + (\mathbf{u}_0^* \mathbf{S}_2 + \mathbf{u}_1^* \mathbf{S}_1 + \mathbf{u}_2^* \mathbf{S}_0) \boldsymbol{\Phi} \boldsymbol{\Omega}^4 \\ & + (\mathbf{u}_0^* \mathbf{S}_3 + \mathbf{u}_1^* \mathbf{S}_2 + \mathbf{u}_2^* \mathbf{S}_1 + \mathbf{u}_3^* \mathbf{S}_0) \boldsymbol{\Phi} \boldsymbol{\Omega}^6 \big] \boldsymbol{\eta}. \end{aligned} \tag{80}$$

Equation (79) is the generalization of a traditional procedure for prescribed nodal displacements in dynamic analysis [1]. However, convergence with mesh refinement is very weak, as rigid body displacements are only approximately represented. An improved formulation is being currently investigated [13].

8. Numerical examples

8.1. Finite element analysis of a fixed-free bar

Consider a fixed-free, uniform bar subjected to a sudden application of constant axial force at the free end. The bar is discretized with six equally spaced elements. Figure 1 shows the displacement response of the free end with time, considering 1 to 4 frequency terms and taking into account all $n = 6$ vibration modes in each solution, in order to demonstrate the improvement in accuracy [9]. The results are normalized with respect to the static response. Geometry and mechanical properties of the bar are the same as in the second example, and are given in Fig. 2. The target results come from the analytical solution of the problem with 100 terms of the series. In all cases, time integration has been performed using Duhamel's integral.

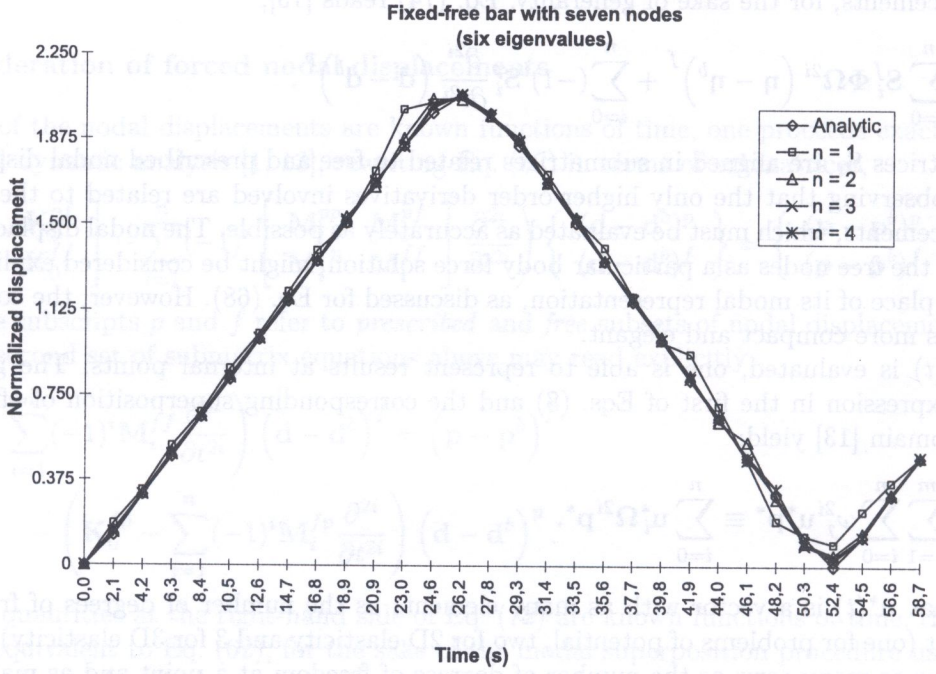

Fig. 1. Displacement response at the end of a fixed-free bar subjected to a step-function axial load

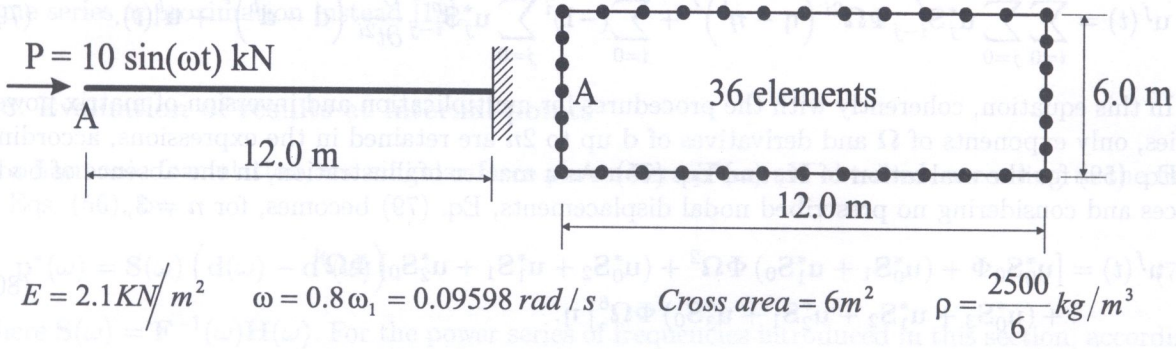

Fig. 2. Fixed-free bar submitted to a periodic load at its free end. The structure is discretized with 36 linear elements

8.2. Boundary element analysis of a fixed-free bar

Figure 2 illustrates a fixed-free bar submitted to a periodic load at its free end. The circular frequency is 80% of the first natural frequency. The 12m×6m rectangular structure is analyzed as a two-dimensional potential problem with 36 linear boundary elements, as indicated in Fig. 2, for constant unity thickness [9]. The normalized displacement response of node A is given in Fig. 3.

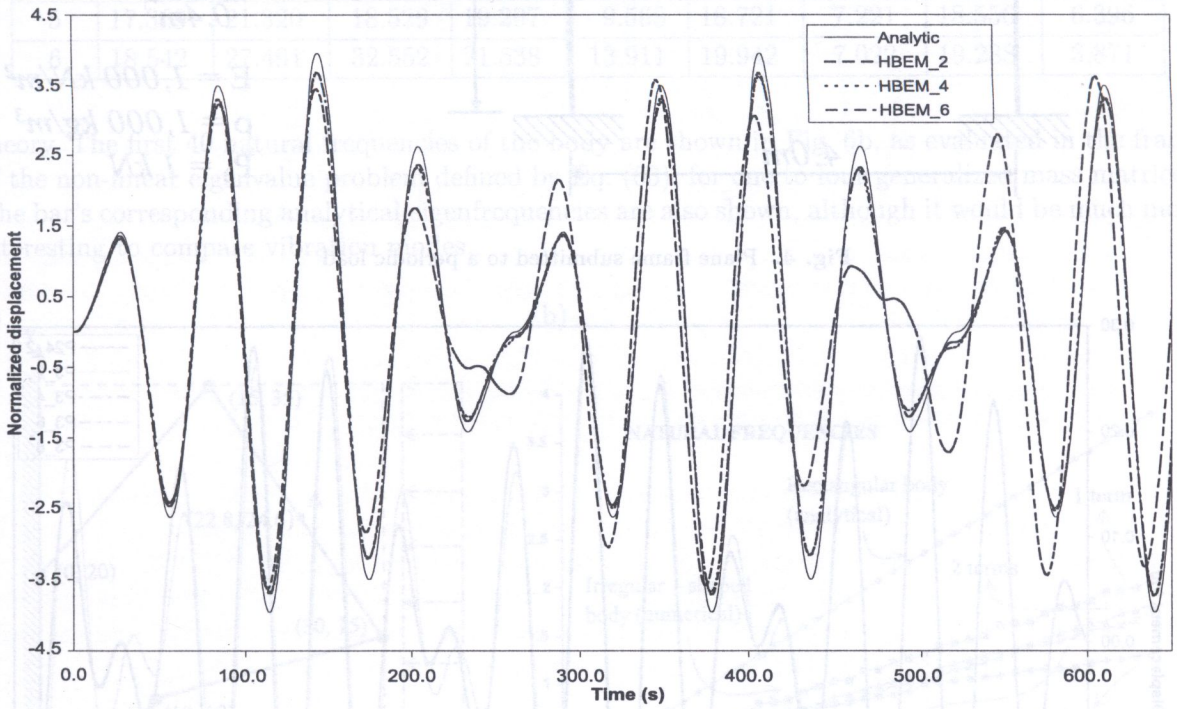

Fig. 3. Normalized displacement response of node A of the fixed-free bar in Fig. 2 as compared with the analytical solution

Cases with one, two and three frequency terms were considered, as labeled as HBEM_2, HBEM_4 and HBEM_6 in Fig. 3, respectively. Note how additional frequency terms dramatically improve the results. However, the mesh discretization used should yield still better results, for an implementation with higher-order boundary elements.

8.3. Plane frame subjected to a periodic load

Figure 4 illustrates a plane frame subjected to a horizontal periodic force. A target analysis was performed using a total of 24 beam elements with traditional, frequency-independent mass and stiffness matrices. Then, the analysis was repeated using only three beam elements for the frame, initially with frequency-independent mass and stiffness matrices, and subsequently adding frequency-dependent terms, according to Eq. (61). The first six free-vibration frequencies of this plane frame are given in Table 1, as evaluated through Eq. (63) for the different models. The models are characterized as Px_y, in which x is the total number of elements and y is the highest frequency power in the series expansion of the generalized mass matrix. Note the extreme accuracy of the frequency values for the model P3_8. The displacement response of the point of application of the periodic force is shown in Fig. 5 for each one of the discretized models. The results with higher frequency terms, for a discretization with only 6 degrees of freedom, almost coincide with the target solution, which has been carried out using 69 degrees of freedom [9].

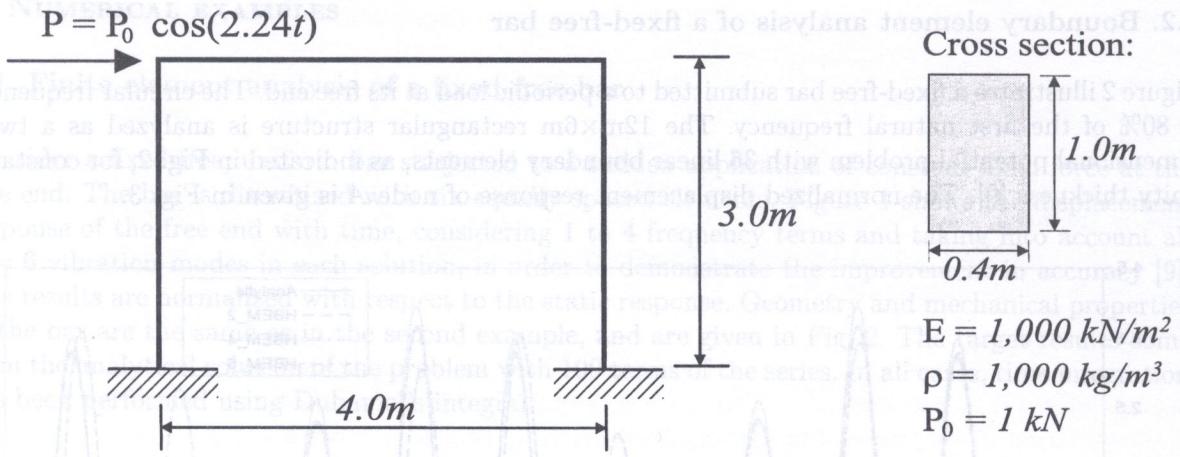

Fig. 4. Plane frame submitted to a periodic load

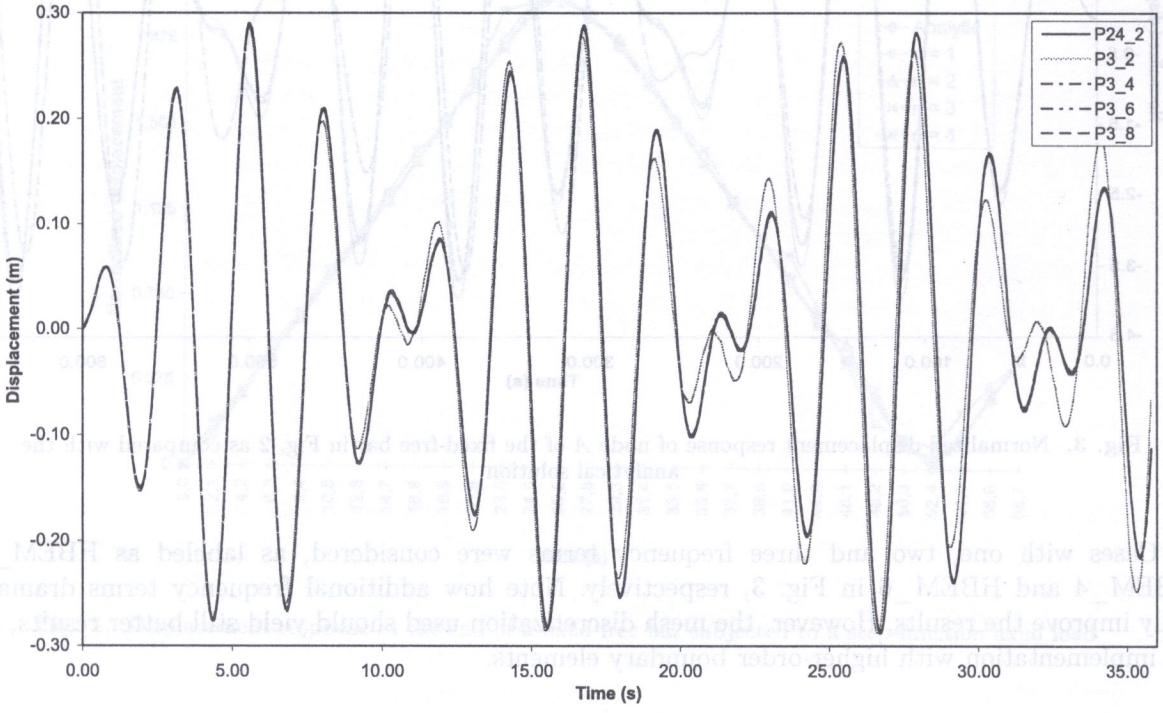

Fig. 5. Displacement response of the point of application of the periodic load of Fig. 4

8.4. A patch test illustration

As a simple academic example, consider the $30 \times 35 \times 1$ solid, fixed-free elastic body (wide bar element) of Fig. 6a submitted to a pulsating load of total intensity $P(t) = 10\sin(1.35\omega_0 t)$, in which $\omega_0 = 0.04799$ is the first natural frequency [5]. An irregular-shaped, clamped elastic body, as illustrated, is cut out of the bar element and subsequently submitted to time-dependent tractions along its boundaries, as evaluated from the bar's analytical response along the cutting lines. This configures a patch test that the pioneer Irons possibly never dreamt of. The simple bar's excitation becomes, for a ten-term series expansion, a very complicated set of equivalent, time-dependent nodal loads applied to the irregular body, which is then discretized, in this example, with a total of 94 linear, (almost) equally spaced boundary elements. Owing to the one-dimensional character of the excitation (Poisson's ratio equals zero), this problem can be solved in the frame of the potential

Table 1. Natural vibration frequencies of the plane frame of Fig. 4

Freqs	P24_2	P3_2	Error %	P3_4	Error %	P3_6	Error %	P3_8	Error %
1	2.8197	2.8330	0.467	2.8198	0.000	2.8196	0.006	2.8196	0.006
2	7.1035	8.2179	13.561	7.3454	3.293	7.1696	0.923	7.122	0.272
3	12.959	13.598	4.701	13.030	0.546	12.963	0.030	12.954	0.043
4	14.357	16.266	11.736	14.867	3.429	14.529	1.178	14.418	0.417
5	17.369	21.320	18.529	19.207	9.568	18.721	7.221	18.556	6.396
6	18.542	27.491	32.552	21.538	13.911	19.942	7.022	19.288	3.871

theory. The first 40 natural frequencies of the body are shown in Fig. 6b, as evaluated in the frame of the non-linear eigenvalue problem defined by Eq. (63), for one to four generalized mass matrices. The bar's corresponding analytical eigenfrequencies are also shown, although it would be much more interesting to compare vibration modes.

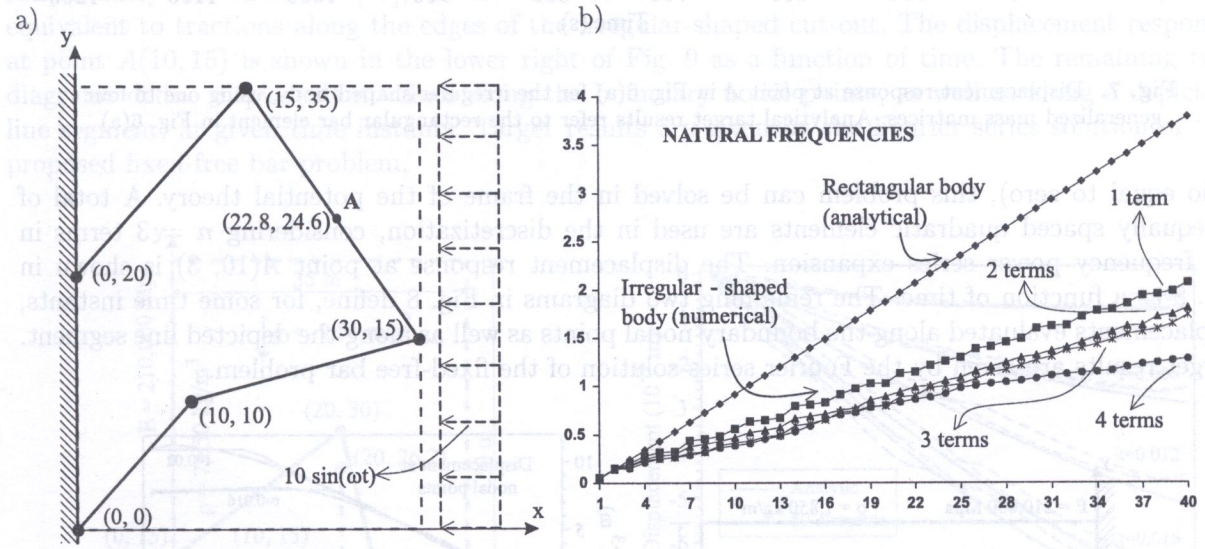

Fig. 6. a) Irregular-shaped body cut out of a truss element, for a patch test; b) first 40 natural frequencies of the irregular shaped body discretized with 94 linear boundary elements, as calculated with one to four generalized mass matrices

In Fig. 7, the displacement of point A in Fig. 6a, normalized with respect to the static displacement response of the bar's free extremity (for $P = 10$), is displayed for a time window $300 - 1200$ seconds. Duhamel's integral has been used for evaluating both the analytical response for point A belonging to the bar element and the numerical response for the same point A on the boundary of the irregular-shaped body, according to the uncoupled Eq. (67) corresponding to the coupled set of Eqs. (62) considering again one to four generalized mass matrices. Owing to the applied fractional frequency of the loading, no periodicity in the structure's response can be perceived in the time window considered. Moreover, as point A is not at the free extremity, a chaotic displacement pattern occurs from time to time, which makes this test a very critical one concerning accuracy of results.

8.5. Consideration of uniform initial velocity in a fixed-free bar

As another simple academic example, consider the fixed-free elastic body (wide bar element) in Fig. 8 submitted to no external loads, but with a prescribed, uniform initial velocity v_0, thus simulating a bar impacting a rigid wall [3]. Owing to the one-dimensional character of the excitation (Poisson's

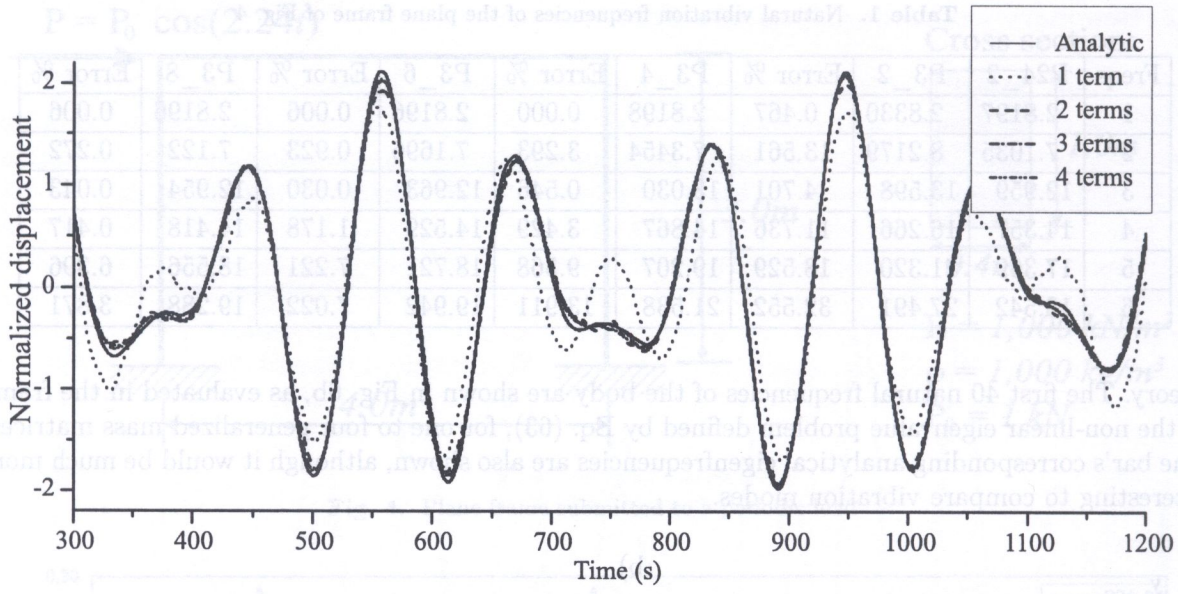

Fig. 7. Displacement response at point A in Fig. 6(a) for the irregular-shaped body, using one to four generalized mass matrices. Analytical target results refer to the rectangular bar element in Fig. 6(a)

ratio equal to zero), this problem can be solved in the frame of the potential theory. A total of 34 equally spaced quadratic elements are used in the discretization, considering $n = 3$ terms in the frequency power series expansion. The displacement response at point $A(10, 3)$ is shown in Fig. 8 as a function of time. The remaining two diagrams in Fig. 8 define, for some time instants, displacements evaluated along the boundary nodal points as well as along the depicted line segment. Target results are given by the Fourier series solution of the fixed-free bar problem.

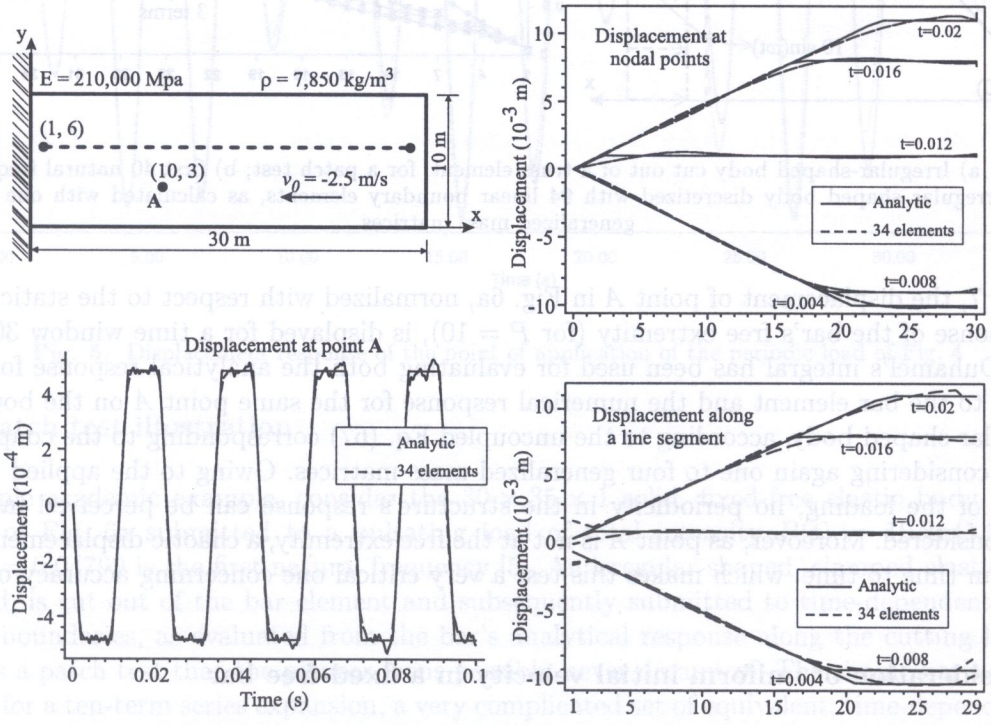

Fig. 8. Fixed-free bar submitted to a constant initial velocity v_0. Displacements are displayed at a nodal point as a function of time and both along all nodal points and along an internal line segment, at some time instants

8.6. Application of sudden gravity acceleration to an irregular-shaped body

A similar example [3] is used for the sudden application of constant gravity acceleration, for homogeneous initial conditions. An irregular-shaped, elastic body, as illustrated in Fig. 9, is cut out of the bar element and subsequently submitted to both time-dependent tractions along the free boundary edges, as evaluated from the bar's analytical response along the cutting lines, and body forces. The body force particular solution of Eq. (6) is $\sigma_y^b = -\rho g(l-y)$, leading to the displacement response $u_y^b = -\rho g(l-y)^2/2E$, in which l is the bar length, g is the acceleration of gravity and E is the elasticity modulus. Although both the analytical problem and the adopted particular solution are extremely simple, the present patch test is a rigourous one, as the excitation of the simple bar becomes a very complicated set of equivalent, time-dependent nodal excitations applied to the irregular body, which is discretized, in this example, with a total of 59 linear, equally spaced boundary elements, for $n = 3$ terms in the frequency power series expansion. This problem is also solved in the frame of the potential theory. The analytical solution for the fixed-free bar element is expressed as a truncated series, as usual. However, a better solution would be piece-wise defined, close-form simple analytical functions [13], so that no errors occur in the evaluation of the nodal forces $\mathbf{p}$ equivalent to tractions along the edges of the irregular-shaped cut-out. The displacement response at point $A(10, 15)$ is shown in the lower right of Fig. 9 as a function of time. The remaining two diagrams define displacement values along the boundary nodal points, as well as along a depicted line segment, at given time instants. Target results are given by the Fourier series solution of the proposed fixed-free bar problem.

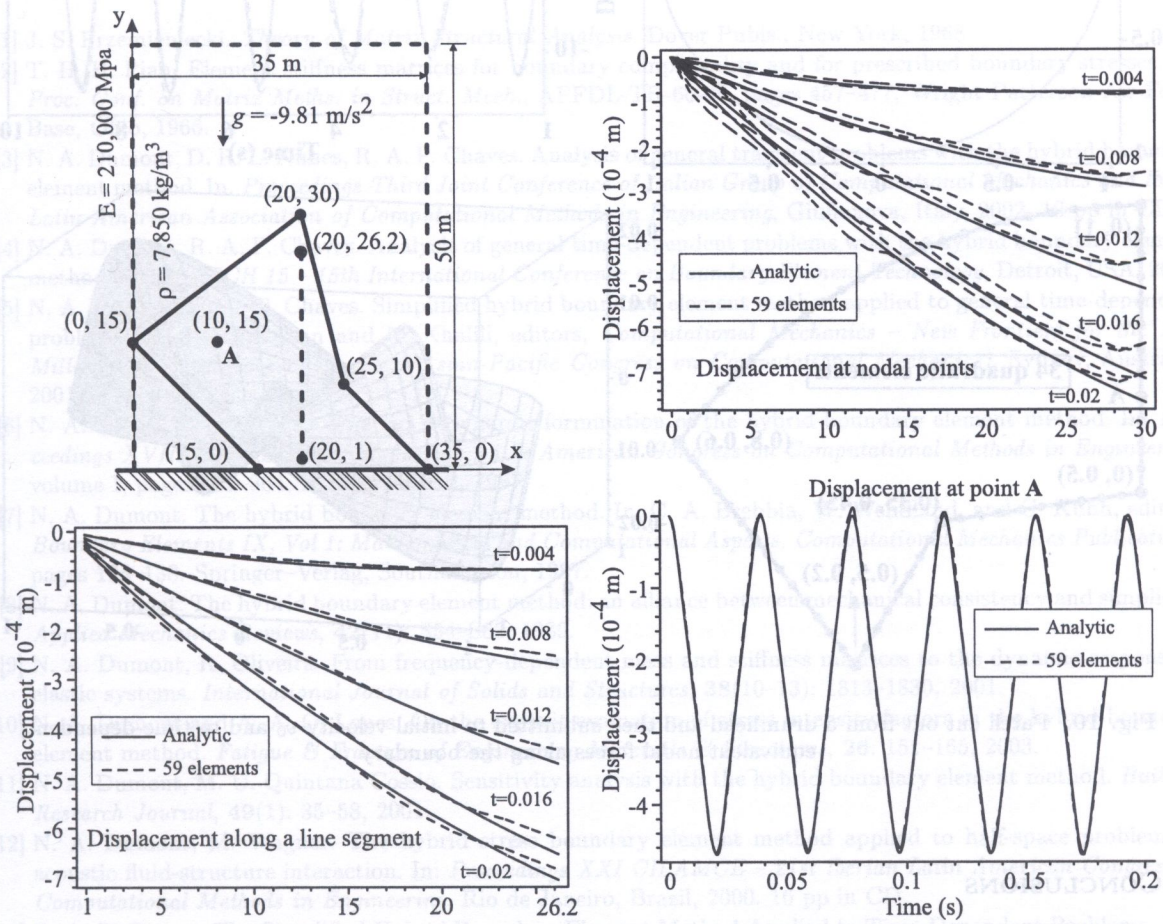

Fig. 9. Patch test for a fixed-free bar submitted to sudden gravity acceleration. Displacements displayed at a nodal point as a function of time and along both nodal points and an internal line segment defined by the dashed line, at some time instants

8.7. Cutout of a drumhead submitted to initial velocity

Consider the evaluation of the displacements of a circular drumhead, as shown in Fig. 10, submitted to initial velocity $v_0 = (r-1)\sin(\theta)$ [4]. This problem can be solved in the frame of the potential theory [20], as illustrated in the snapshot in Fig. 10. As a simple academic exercise, a patch is cut out and discretized with a total of 34 equally spaced quadratic elements. Zero displacements are prescribed along the drumhead's curved edge. Time-dependent, equivalent nodal forces, as evaluated for the solution of the whole circular region, are applied at the remaining boundary nodes. The displacement response at nodal point A is shown in Fig. 10 as a function of time, as evaluated for $n = 3$ terms in the frequency power series expansion of Section 7.3, and compared with results obtained from the analysis of the drumhead as a whole, given as a series of Bessel functions [20]. Improved results may be obtained by considering additional terms in the frequency power series [13].

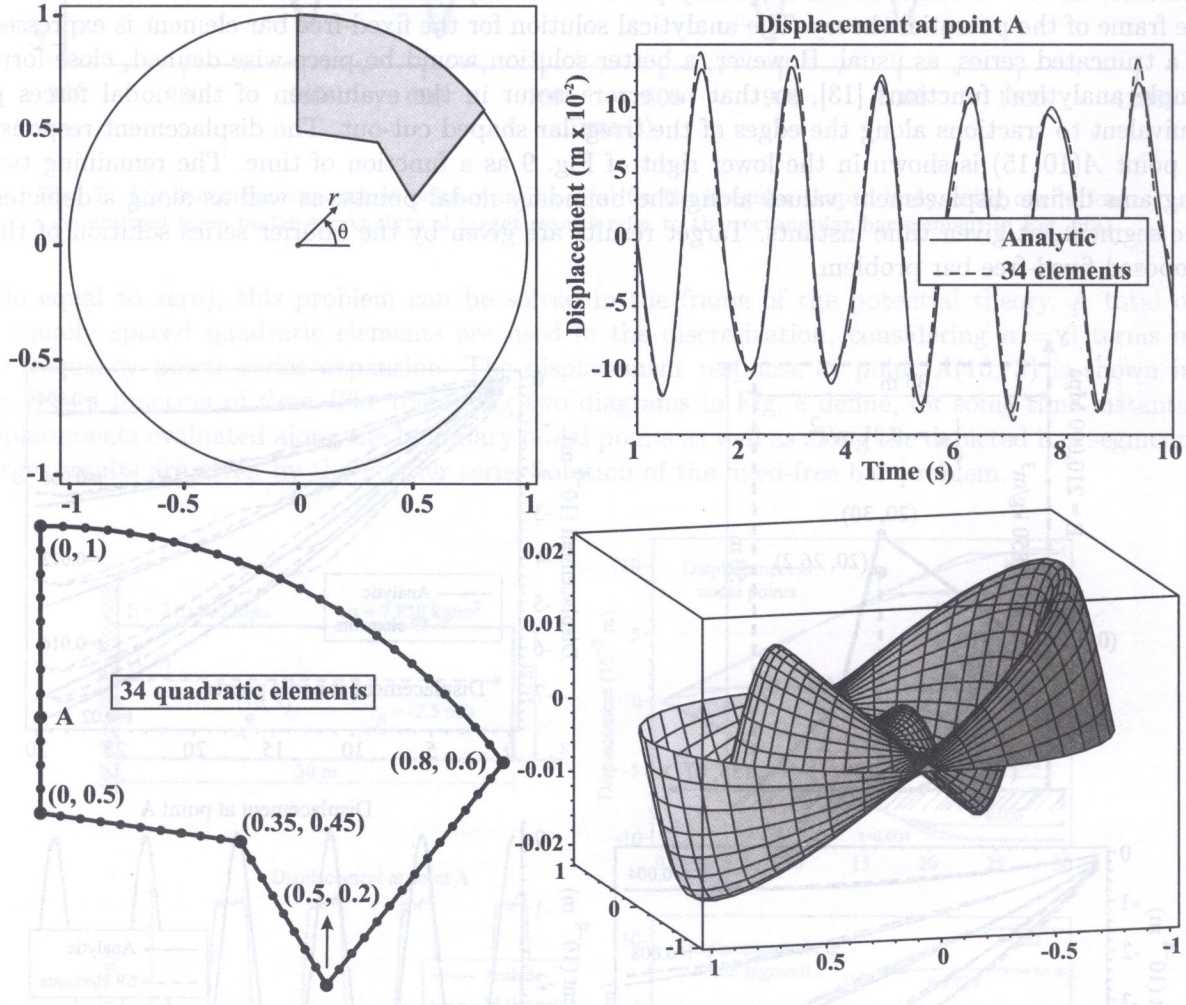

Fig. 10. Patch cut out from a drumhead and then submitted to initial velocity v_0 and to time-dependent, equivalent nodal forces along the boundary

9. Conclusions

The frequency-domain formulation of the hybrid boundary element method is presented for the analysis of general time-dependent problems. The method relies on a power series expansion in the frequency with evaluation of the dynamic response by means of a generalized mode superposition

procedure. The power series expansion ensures that the dynamic differential equilibrium equation is accurately satisfied in the domain, although no internal points or cells are used, as in the conventional boundary element method. It is also worth mentioning that the whole formulation relies on real functions, which is an additional, remarkable advantage. Moreover, evaluation of results at internal points is given directly by a series summation, which simplifies post-processing. Accuracy is as high as and possibly higher than, in other boundary element methods. This frequency-domain formulation and the outlines concerning non-homogeneous initial conditions, forced nodal displacements and applied domain forces applies to finite elements as well. Owing to space restrictions, the numerical results cannot be sufficiently discussed. However, their quality is evident, particularly for the rather demanding patch tests. Additionally, the paper outlines the simplified hybrid boundary element method, which circumvents the time consuming evaluation of the flexibility matrix $\mathbf{F}(\omega)$, thus making all calculations still more advantageous.

Acknowledgments

This project was supported by the Brazilian agencies FAPERJ and CNPq. The authors would like to thank the reviewers for their valuable suggestions, which have greatly improved the manuscript presentation.

References

[1] J. S. Przemieniecki. *Theory of Matrix Structural Analysis.* Dover Publs., New York, 1968.

[2] T. H. H. Pian. Element stiffness matrices for boundary compatibility and for prescribed boundary stresses. In: *Proc. Conf. on Matrix Meths. in Struct. Mech.*, AFFDL-TR-66-80, pages 457–477, Wright Patterson Air Force Base, Ohio, 1966.

[3] N. A. Dumont, D. R. L. Nunes, R. A. P. Chaves. Analysis of general transient problems with the hybrid boundary element method. In: *Proceedings Third Joint Conference of Italian Group of Computational Mechanics and Ibero-Latin American Association of Computational Methods in Engineering*, Giulianova, Italy, 2002. 10 pp in CD.

[4] N. A. Dumont, R. A. P. Chaves. Analysis of general time-dependent problems with the hybrid boundary element method. In: *BETECH 15 - 15th International Conference on Boundary Element Technology*, Detroit, USA, 2003.

[5] N. A. Dumont, R. A. P. Chaves. Simplified hybrid boundary element method applied to general time-dependent problems. In: S. Valliappan and N. Khalili, editors, *Computational Mechanics - New Frontiers for the New Millenium (Proceedings of the First Asian-Pacific Congress on Computational Mechanics)*, Sydney, Australia, 2001. Elsevier Science Ltd.

[6] N. A. Dumont, R. Oliveira. The exact dynamic formulation of the hybrid boundary element method. In: *Proceedings XVIII CILAMCE - 18th Iberian Latin American Congress on Computational Methods in Engineering*, volume I, pages 357–364, Brasília, Brazil, 1997.

[7] N. A. Dumont. The hybrid boundary element method. In: C. A. Brebbia, W. Wendland, and G. Kuhn, editors, *Boundary Elements IX, Vol 1: Mathematical and Computational Aspects, Computational Mechanics Publications*, pages 125–138. Springer–Verlag, Southampton, 1987.

[8] N. A. Dumont. The hybrid boundary element method: an alliance between mechanical consistency and simplicity. *Applied Mechanics Reviews*, **42**(11): S54–S63, 1989.

[9] N. A. Dumont, R. Oliveira. From frequency-dependent mass and stiffness matrices to the dynamic response of elastic systems. *International Journal of Solids and Structures*, **38**(10–13): 1813–1830, 2001.

[10] N. A. Dumont and A. A. O. Lopes. On the explicit evaluation of stress intensity factors in the hybrid boundary element method. *Fatigue & Fracture of Engineering Materials & Structures*, **26**: 151–165, 2003.

[11] N. A. Dumont, M. U. Quintana Cossio. Sensitivity analysis with the hybrid boundary element method. *Building Research Journal*, **49**(1): 35–58, 2001.

[12] N. A. Dumont, M. Wagner. The hybrid stress boundary element method applied to half-space problems in acoustic fluid-structure interaction. In: *Proceedings XXI CILAMCE - 21st Iberian Latin American Congress on Computational Methods in Engineering*, Rio de Janeiro, Brazil, 2000. 16 pp in CD.

[13] R. A. P. Chaves. The Simplified Hybrid Boundary Element Method Applied to Time-Dependent Problems. *PhD thesis* (in Portuguese), PUC-Rio, Brazil, 2003.

[14] R. A. P. Chaves. Study of the hybrid boundary element method and proposal of a simplified formulation. *Master's thesis* (in Portuguese), PUC-Rio, Brazil, 1999.

[15] N. A. Dumont, R. A. P. Chaves. The simplified hybrid boundary element method. In: University of Colorado, editor, *Book of Abstracts 5th U.S. National Congress on Computational Mechanics*, pages 68–69, Boulder, USA, 1999.

[16] N. A. Dumont, R. A. P. Chaves. The simplified hybrid boundary element method. In: *Proceedings XX CILAMCE – 20th Iberian Latin American Congress on Computational Methods in Engineering*, Sao Paulo, Brazil, 1999. 20 pp in CD.

[17] R. A. P. Chaves, N. A. Dumont. The simplified hybrid boundary element method applied to frequency-domain problems. In: *Proceedings XXI CILAMCE – 21st Iberian Latin American Congress on Computational Methods in Engineering*, Rio de Janeiro, Brazil, 2000. 20 pp in CD.

[18] N. A. Dumont. An assessment of the spectral properties of the matrix **G** used in the boundary element methods. *Computational Mechanics*, **22**(1): 32–41, 1998.

[19] N. A. Dumont. Variationally-based, hybrid boundary element methods. In: A. A. Javadi, E. A. W. Maunder, eds., *Proceedings 3rd International Conference/Euro Workshop on Trefftz Methods*, page 25 pp in CD, Exeter, England, 2002.

[20] M. L. Abell, J. P. Braselton. Differential equations with Maple V. *AP Professional*, New York, 1994.